



---

## Modeling and Simulation of a Grid-Connected Three-Phase Photovoltaic Inverter with Integrated Voltage Stabilization for Residential Applications

Ayman R. Khaled Saed

Electrical Engineering Department, Faculty of Engineering, Tobruk University, Tobruk, Libya.  
Ayman.saed@tu.edu.ly

---

**Received:** Nov 2, 2025; **Accepted:** Dec 20, 2025

---

**Abstract**—Effective inverter design is necessary for photo-voltaic system integration into power grids in order to guarantee power quality and standard compliance. In this paper, a three-phase grid connected PV inverter is modeled and simulated using MATLAB/Simulink. Equations that depend on temperature and irradiance are used to model the PV, and its output is stabilized before being fed into a three leg IGBT inverter. Maximum power point tracking (MPPT) optimizes energy extraction, while an LC filter and phase locked loop are used to produce sinusoidal output and grid synchronization. With the root mean square output voltage of 230 V and a total harmonic distortion (THD) of 2.2%, simulation results verify steady operation at 10 kW, satisfying International Electrotechnical Commission (IEC) requirements. The recommended design works faithfully and is proper for small-scale industrial and residential applications.

**Keywords**—PV inverter; Grid-connected systems; Simulink; MPPT; THD

---

### 1. Introduction

In many countries, pollution remains a major environmental and public health challenge, and energy generation has a significant influence on it. The air quality can be very low in some urban and industrial areas. The more carbon dioxide we release into the atmosphere, the greater the effect of air pollution and global warming becomes. Current climate valuations emphasize that reducing emissions from the power sector is essential to reach an international climate target and improving urban air quality [1].

By making renewable energy easy to use and economically profitable, we can reduce the use of fossil fuels. The Photovoltaic (PV) provide cost-effective solutions for industrial and domestic applications supported by declining installation costs and increasing efficiency. The topical matters of air pollution and global warming are crucial importance, and their resolution requires corresponding efforts from researchers and engineers, beside social acceptance and institutional funding. In the design of inverters for PV-grid systems, the DC voltage generated by the PV array must be converted into a suitable AC voltage. Tracking the maximum power point (MPPT) enables maximization of the exploited energy under varying irradiance and temperature conditions.

Furthermore, the current injected into the grid should comply with international regulations such as EN61000-3-2 and IEEE 1547, which specify permissible levels of injected harmonics and other interconnection parameters to ensure power quality and grid are stable [2].

Since the task is the design of power electronics applications, such as PV inverters, simulation programs are a useful asset. They provide the option to control and visualize the system's dynamic behavior. Such programs are MATLAB/Simulink, OrCAD PSpice, etc. Simulink has the basic advantage of being especially built to develop and control continuous–discrete time systems and use transfer functions [3]. The PV industry has the need for more sophisticated inverter design to enhance their functionality, reduce cost, and suit new proposed topologies [4,5].

In this paper we will study the simulation behavior of a 3-phase grid-connected PV inverter that has the ability to feed a load of 10 kW. This value of load has been chosen because it fits the average energy used by an ordinary household and other professional buildings. We assume that the surface that the PV array will virtually cover is about 72m<sup>2</sup>. Such a size can be accommodated and installed on a roof, as well as providing to the load the appropriate amount of energy [6].

## 2. PV Array

### 2.1 Factors affecting PV module efficiency

The major factors that affect the efficiency of a PV module are the temperature and the solar radiation. The PV cell output voltage ( $V_c$ ) is a function of the photocurrent determined by the load current and the solar irradiation level during operation. An analytical approximation providing an overview of key parameters can be summarized as [5]:

$$V_c = \frac{AkT_c}{e} \ln\left(\frac{I_{ph} + I_o - I_c}{I_o}\right) - R_s I_c \quad (1)$$

Temperature correction factors for voltage and current, respectively:

$$C_{TV} = 1 + B_T (T_c - T_x) \quad (2)$$

$$C_{TI} = 1 + \frac{Y_T}{S_c} B_T (T_c - T_x) \quad (3)$$

Irradiance correction factors for voltage and current, respectively,

$$C_{SV} = 1 + Y_T (S_x - S_c) \quad (4)$$

$$C_{SI} = \frac{S_x}{S_c} \quad (5)$$

Applying the correction factors:

$$V_{cx} = V_c C_{TV} C_{SV} \quad (6)$$

$$I_{phx} = I_{ph} C_{TI} C_{SI} \quad (7)$$

Combining (1), (6), and (7) yields the MPP locus; MPP tracking (MPPT) can be executed in the control unit micro-controller using a feedback procedure at appropriate frequency [7].

Where,  $e$ : Electron charge (C) ,  $k$ : Boltzmann constant (J/K),  $I_c$ : Cell output current (A),  $I_{ph}$ : Photocurrent (A),  $R_s$ : Series resistance of one cell ( $\Omega$ ),  $T_c$ : Standard test condition (STC) temperature (K),  $V_c$ : Cell output voltage (V),  $A$ : Curve fitting factor (dimensionless),  $B_T$ : Temperature correction coefficient (1/K),  $Y_T$ : Irradiance correction coefficient ( $W/K \cdot m^2$ ),  $\alpha_s$ : Irradiance-related slope or scaling factor ( $K \cdot m^2/W$ ),  $T_x$ : Ambient temperature (variable) (K),  $S_c$ : STC irradiance ( $W/m^2$ ),  $S_x$ : Variable irradiance ( $W/m^2$ ),  $(\frac{Y_T}{S_c})$  The ratio indicates the correlation between the rated load current  $S_c$  and the current-dependent factor  $Y_T$ .

## 2.2 Simulation of the PV array

According to market data, achieving a DC bus voltage of approximately 700 V at 15 A requires the use of 60 monocrystalline silicon modules, arranged as three parallel strings of 20 series-connected panels each. The selected module is the FVG 72-125 (FVG 185M-MC) manufactured by FVG ENERGY (Italy), with a rated peak power of 185 W, a cell efficiency of 17.5%, and a module efficiency of 14.6%.

The PV array was modeled and simulated in MAT-LAB/Simulink using hourly meteorological data over a one-year period, with the array-oriented south, tilted at  $36^\circ$ , and covering surface  $72 \text{ m}^2$ . The total simulated annual energy yield was 8502 kWh.

As expected, the output characteristics varied with temperature, irradiance, and time of day. Predictive approaches for estimating PV energy production can be further enhanced by combining long-term simulation with short-term morning measurements [8].

Maximum Power Point tracking plays a crucial role in solar utilization by keeping the DC operating point at maximum power; it can be computed from functions like (1) in the control microprocessor [7].

## 2.3 Inverter and stabilizer topology

The proposed grid-connected PV inverter topology consists of: (1) PV array generating DC; (2) stabilizer regulating PV voltage to feed the inverter and support MPPT; (3) three-phase inverter converting DC to AC; (4) LC low-pass filter to attenuate high-frequency harmonics; (5) control unit with Phase-Locked Loop (PLL) to synchronize inverter phase to the grid and PWM to switch IGBTs [9].

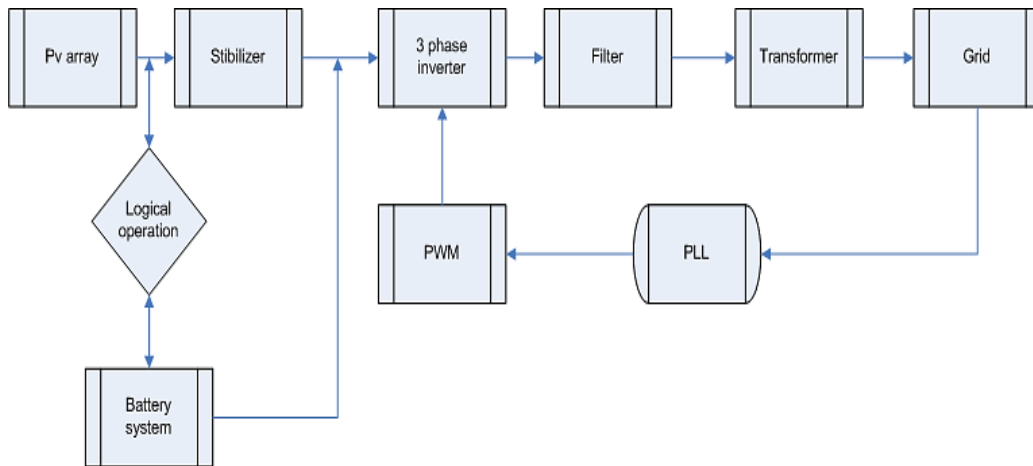


**Figure 1.** Block diagram of the topology used (PV array, stabilizer, 3-phase inverter, LC filter, control unit, transformer, grid)

The stabilizer regulates  $\sim 700\text{V}$  PV output to  $\sim 650\text{V}$  using a four-IGBT bridge and two switches that compare output to the  $650\text{ V}$  target and command IGBTs accordingly via a sync signal. A low-pass LC filter follows and feeds the inverter. A buck converter alternative was also tested. Improving stabilizer functionality to regulate regardless of irradiance, cell efficiency, and MPPT voltage is necessary, as these factors affect generated power and thus AC voltage amplitude; integration with PWM control can maximize efficiency [4].

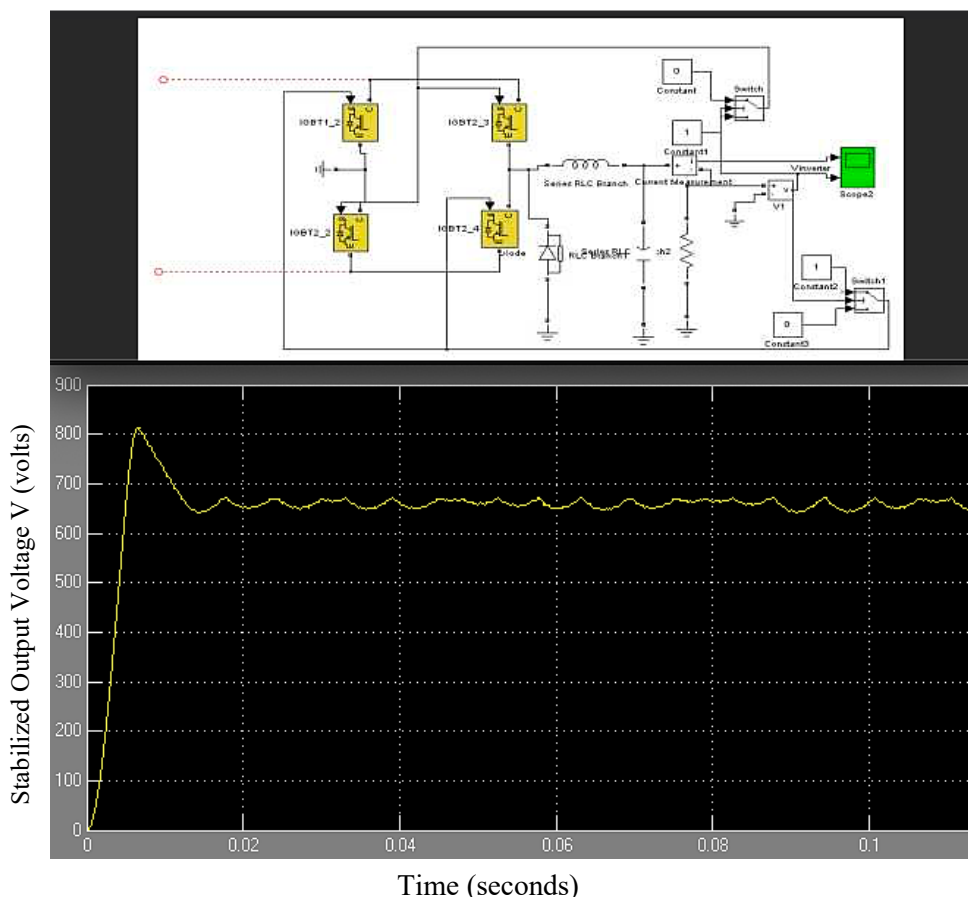


**Figure 2.** Stabilizer Simulink block diagram and stabilized output voltage (V).

The main inverter is a three-leg, six-IGBT bridge with a control unit generating gate pulses. PWM at  $\sim 1$  kHz drives the switches; during on-time, pulses of DC bus amplitude appear at the power circuit, and RMS time integration yields AC outputs. The modulation index  $m_a$  serves as a dynamic control parameter to correct grid voltage fluctuations arising from PV and MPPT; with losses scaling according to variations in  $m_a$ . The discussion considers multilevel alternatives and associated control strategies. Three-phase operation ensures robust and reliable power conversion [9,10].

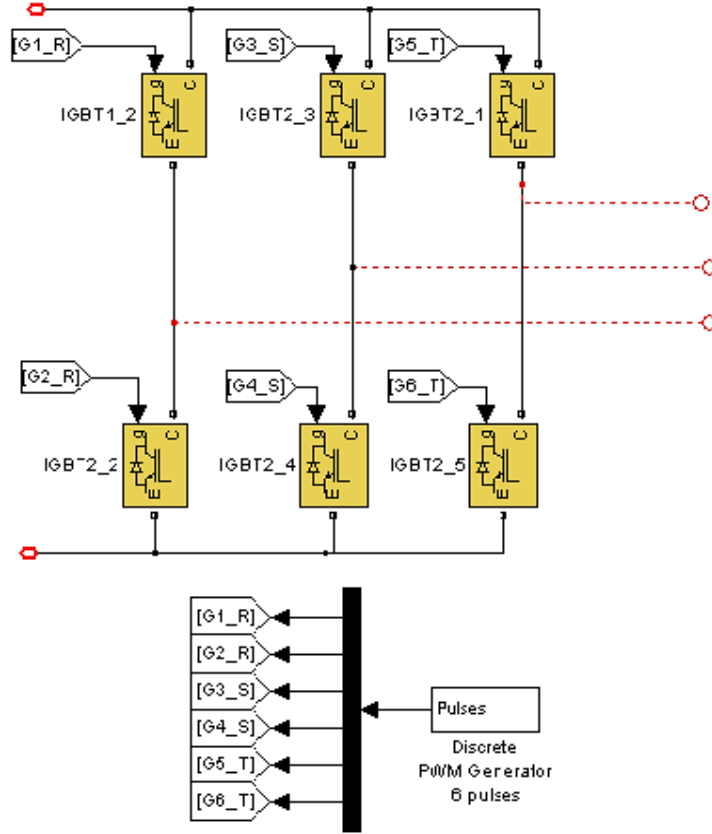


**Figure 3.** Inverter simulation (gating signals)

Considering one inverter phase leg with LC filter  $L$ ,  $C$  and resistive load  $R$ , applying Kirchhoff's laws (IGBTs open-state averaged model) yields [6]:

$$Ri_L + L \frac{di_L}{dt} + v_c = V_o(t) \tag{8}$$

$$i_L - C \frac{dv_c}{dt} = 0 \tag{9}$$

Where,  $R$ : resistance of the inductor ( $\Omega$ ),  $C$ : capacitance (F),  $L$ : inductance (H),  $i_L$ : current flowing through the inductor (A),  $v_c$ : voltage across the capacitor (V);  $V_o$ : output voltage (V).

Matrix form:

$$\frac{dy}{dx} \begin{bmatrix} i_L \\ v_c \end{bmatrix} = \begin{bmatrix} -\frac{R}{L} & -\frac{1}{L} \\ \frac{1}{C} & 0 \end{bmatrix} \begin{bmatrix} i_L \\ v_c \end{bmatrix} + \begin{bmatrix} \frac{1}{L} \\ 0 \end{bmatrix} v_{oi} \tag{10}$$

Simplified as  $\dot{x}(t) = Ax(t) + bg(t)$ , with  $x = [i_L \ v_c]^T$ ,  $g = v_{oi}$  [10].

For the switched leg (space-vector/PWM idealization), the phase-to-neutral voltages contain dominant harmonics  $n = 1, 5, 7, 11, \dots$

$$V_{RN}(t) = \sum_{n=1,5,7} \frac{4V}{n\pi} (\cos \frac{n\pi}{3} + 1) \sin(n\omega t) \quad (11)$$

$$V_{SN}(t) = \sum_{n=1,5,7} \frac{4V}{n\pi} (\cos \frac{n\pi}{3} + 1) \sin(n\omega t - 120^\circ) \quad (12)$$

$$V_{TN}(t) = \sum_{n=1,5,7} \frac{4V}{n\pi} (\cos \frac{n\pi}{3} + 1) \sin(n\omega t - 240^\circ) \quad (13)$$

Simulink solves the full switched nonlinear system numerically, beyond the simplified series above [10].

Where,  $V_{RN}$ ,  $V_{SN}$ ,  $V_{TN}$ : Instantaneous line-to-neutral voltages of phases R, S, and T respectively (volts),  $V$ : Peak amplitude of the voltage (volts),  $n$ : Harmonic order.

## 2.4 Control circuit

The control circuit provides PWM pulses, synchronizes inverter phases to the grid via PLL, and tracks MPPT. Implementation options include a TMS320F2812 DSP [11], and low-cost approaches utilizing audio PWM ICs (Class-D) [12]. Simulink's default control supports sinusoidal waveform extraction by comparing a sinusoidal reference to a sawtooth carrier (classic PWM). The modulation index  $m_a$  (ratio of reference to carrier amplitudes) enables dynamic control [13].

For realistic daily outputs, the grid and the load are modeled: a preliminary house load of  $\sim 10$  kW (high R, small L); grid impedance estimation methods are discussed in [14]. The LC filter values used are  $L = 20\text{mH}$  and  $C = 35\mu\text{F}$ .

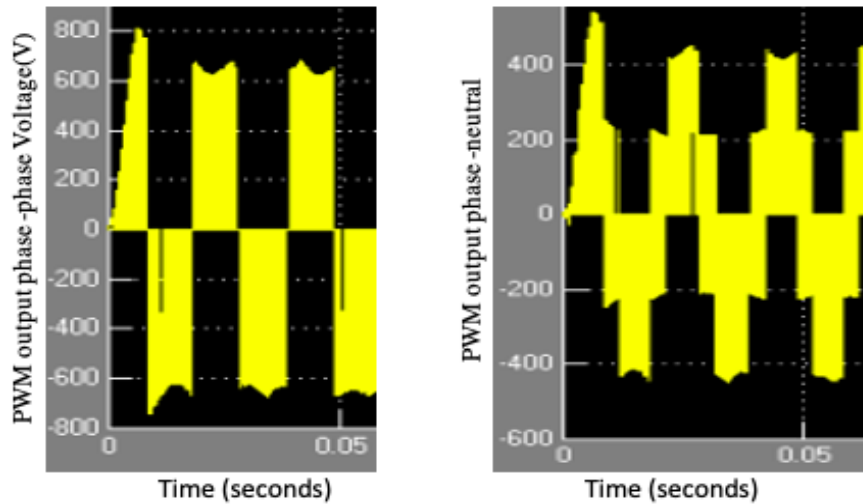


**Figure 4.** The pulse generator and the output Voltage (V) Phase to Phase and Phase-Neutral.

## 3. Analysis and Discussion

From output scopes: phase-to-neutral voltage after LC filtering (upper) and before filtering (lower), corresponding to IGBT pulses, show variations increasing with load from 1 kW to 10 kW; holistic modeling reveals these dynamics, whereas isolated subsystem views look ideal.

Phase-to-phase output voltage waveforms correspond to sinusoidal profiles after filtering; similar variation behavior is observed in the pulse waveforms prior to filtering.

Measured VRMS is  $\approx 230 \pm 5$  V, compliant with regulations; total harmonic distortion (THD) was as low as  $\sim 2.2\%$ , consistent with IEC targets, following system optimization [15]. THD can be further improved using harmonic reduction techniques [10]; transformers and alternative topologies can also reduce THD but introduce losses, cost, and size penalties [15].

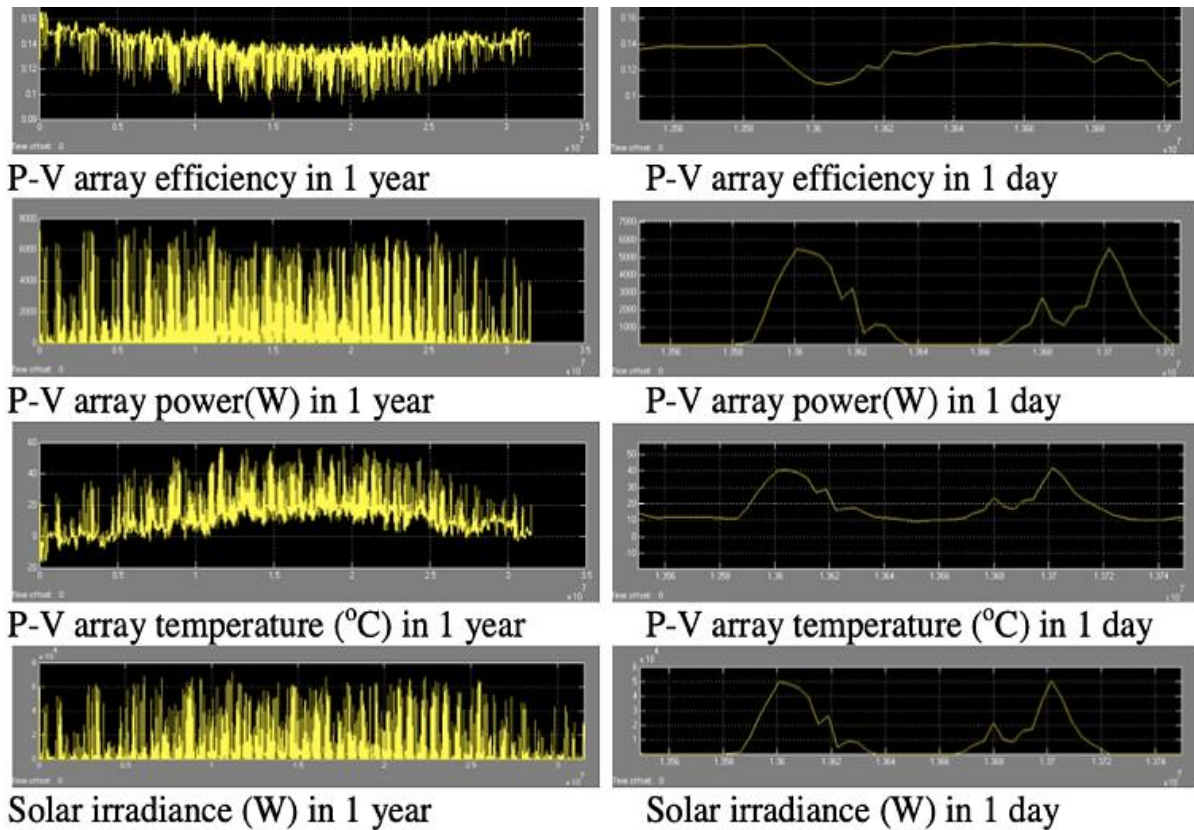


**Figure 5.** Photovoltaic array simulation results. Left: one-year efficiency, power, temperature, irradiance. Right: one/two-day zooms.

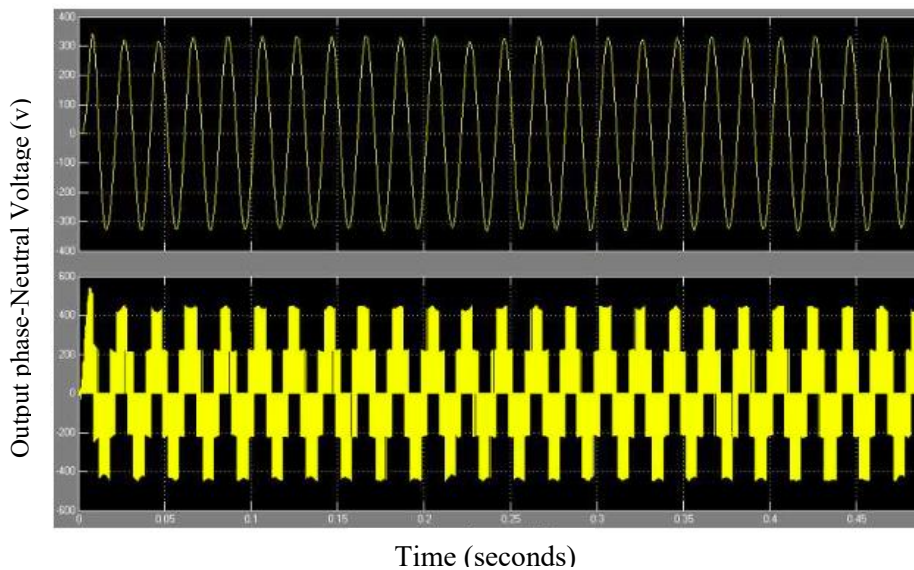


**Figure 6.** Inverter output voltage phase-neutral, shown after filtering (upper trace) and before filtering (lower trace).

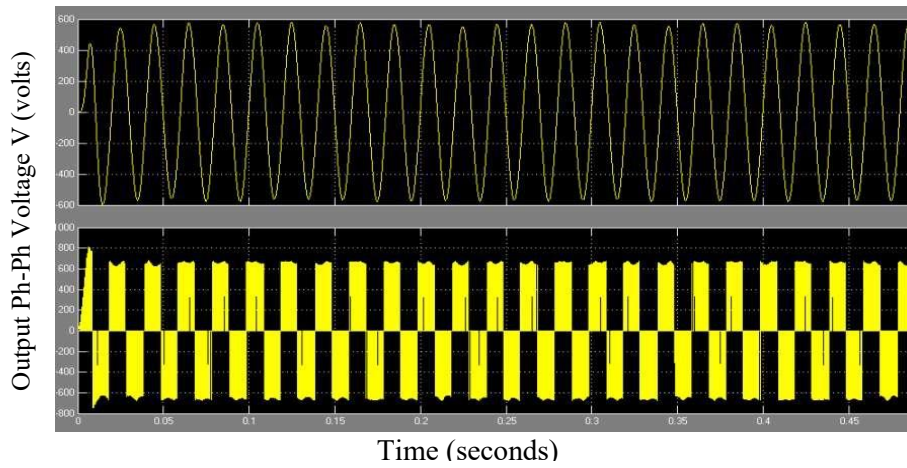


**Figure 7.** Inverter output voltage phase-to-phase, shown after filtering (upper trace) and before filtering (lower trace).

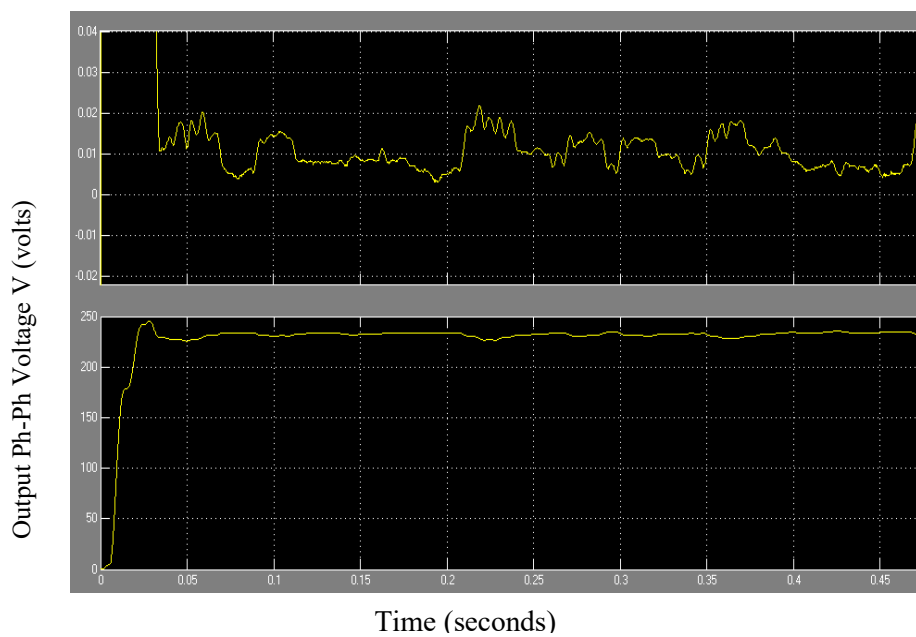


**Figure 8.** Inverter output voltage phase-to-phase, shown after filtering (lower trace) and before filtering (upper trace).

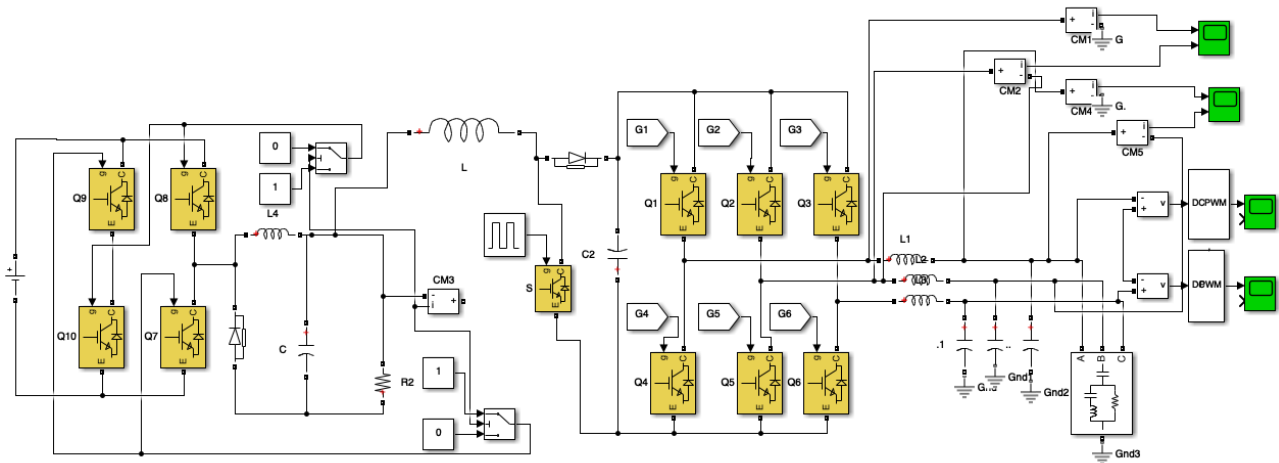


**Figure 9.** Total circuit in Simulink

## 5. Conclusion

This study presented the modeling and simulation of a three-phase grid-connected photovoltaic (PV) inverter in MAT-LAB/Simulink. The PV array, modeled with temperature- and irradiance-dependent equations, was simulated over a one-year period and produced an annual energy yield of 8502 kWh. The integrated system including stabilizer, inverter, LC filter, and control circuits demonstrated stable operation at the rated 10 kW load. Future work should extend the control framework, incorporate real-world implementation studies alongside simulation, and perform cross-validation with circuit-level tools such as PSpice to enhance reliability. Continued development of inverter technology is also required to achieve higher efficiency and compatibility with emerging topologies for PV plants and alternative energy applications, including fuel cells. Meanwhile, single-phase PV inverters remain a strong and practical option for residential deployment.

## Acknowledgment

The author sincerely expresses gratitude to the department of electrical engineering, faculty of engineering, Tobruk University, Libya, for providing the essential facilities, technical guidance, and constructive feedback that greatly supported the development of the manuscript.

## References

- [1] Intergovernmental Panel on Climate Change (IPCC), *Climate Change 2023: Synthesis Report*, Core Writing Team, H. Lee, J. Romero (eds.), Geneva, Switzerland, 2023. doi: 10.59327/IPCC/AR6-9789291691647.
- [2] X. Li, Y. Zhang, H. Wang, "Recent advances in grid-connected photovoltaic inverter technologies: Control, performance, and standards compliance," *IEEE Access*, Vol. 12, 45678–45695, 2024, doi: 10.1109/ACCESS.2024
- [3] S. Orts, S. Segui, F.J. Gimeno, M. Alcañiz, R. Masot, "Modeling and simulation of three-phase power active compensator with Matlab/Simulink," *Annual Power Electronics Specialists Conference, IEEE PESC, Aachen, Germany*, Vol. 4, 3182-3187, 2004.
- [4] L. Castaner, S. Silvestre, "Modeling Photovoltaic Systems Using PSpice," Chichester, U.K., Wiley, 2002.
- [5] I.H. Altas, A.M. Sharaf, "Photovoltaic array simulation model for Matlab-Simulink GUI environment," in *Proc. Int. Conf. Clean Electrical Power, Capri, Italy, IEEE*, 2007.
- [6] M. Ilyas, S. Ali, M.A. Khan, "Modeling and simulation of 10 kW grid-connected PV generation system using MATLAB/Simulink," *International Journal of Electrical and Electronics Engineering*, Vol. 13(24), 16962–16970, 2018.
- [7] M.A.S. Masoum, H. Dehbonei, "Design, construction and testing of a voltage-based maximum power point tracker (VMPPT) for small satellite power supply," in *Proc. 13th AIAA/USU Conf. Small Satellites, Logan, UT, USA*, 1999.
- [8] S.A. Khajehoddin, P. Jain, A. Bakhshai, "Cascaded multilevel converters and their applications in photovoltaic systems," in *Proc. 2nd Canadian Solar Buildings Conf., Calgary, Canada*, 1–6, 2007.
- [9] K. Hayashi, T. Shimada, H. Koizumi, Y. Ohashi, K. Kurokawa, "A new grid-connected inverter by utilizing ready-made PWM ICs for audio power amplifier," in *Proc. 15th Int. PV Science & Engineering Conf., Shanghai, China*, 2005.
- [10] S. Manias, *Power Electronics (Greek Edition)*, Athens, Greece: Symmetria, 2007.

- [11] C. Eduardo, C.A. Petry, S.A. Mussa, H.B. Mohr, "AC indirect line conditioner digital control using PLL based on the three-phase instantaneous power theory," in Proc. IEEE Int. Conf. Industrial Electronics (IECON), Paris, France, 2535–2540, 2006.
- [12] L. Asiminoaei, R. Teodorescu, F. Blaabjerg, U. Borup, "A digital controlled PV inverter with grid impedance estimation for ENS detection," IEEE Trans. Power Electron., Vol. 20(6), 1480–1490, 2005.
- [13] University of New South Wales, "PC1D: Photovoltaic Cell/Module Modeling Software," UNSW, Sydney, Australia, Online link: <https://www2.pvlighthouse.com.au/resources/pc1d>.
- [14] R.H. Bonn, "Developing a next generation PV inverter," in Proc. IEEE Photovoltaic Specialists Conf., 1352-1355, 2002.
- [15] S.B. Kjær, J.K. Pedersen, F. Blaabjerg, "A review of single-phase grid-connected inverters for photovoltaic modules," IEEE Trans. Ind. Appl., Vol. 41(5), 1292–1306, 2005.